iScience, Volume *24*

Supplemental information

Green oxygen power plants in the brain

rescue neuronal activity

Suzan Özugur, Myra N. Chávez, Rosario Sanchez-Gonzalez, Lars Kunz, Jörg Nickelsen, and Hans Straka

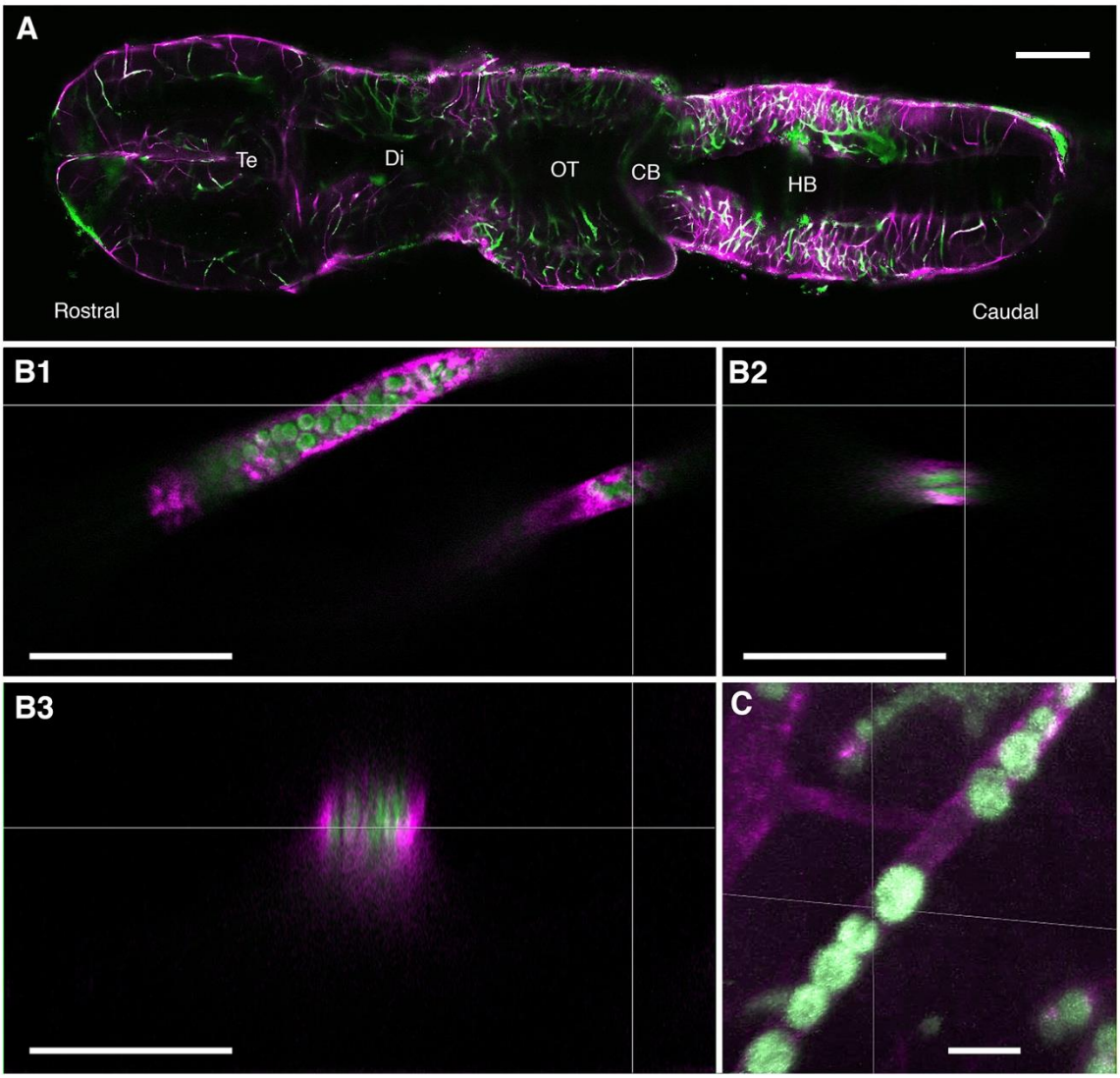

Supplemental fig. S1. Photosynthetic microorganisms in brain blood vessels (Related to Fig. 1G-J). (**A**) Confocal reconstruction of a *Xenopus laevis* whole brain illustrating Isolectin-labeled endothelial walls of blood vessels (magenta) and chlorophyll autofluorescence of transcardially injected *Synechocystis* 6803 (green). (**B, C**) Confocal reconstruction of blood vessels in the hindbrain (B1) and optical sections in orthogonal projection planes (B2, B3), demonstrating the containment of the microorganisms (green; *Synechocystis* 6803 in B, *C. reinhardtii* in C) inside the blood vessels (magenta). Calibration bars represent 1 mm (a), 20 µm (B1-3) and 10 µm (C); Te, telencephalon; Di, diencephalon; OT, optic tectum; CB, cerebellum; HB, hindbrain.

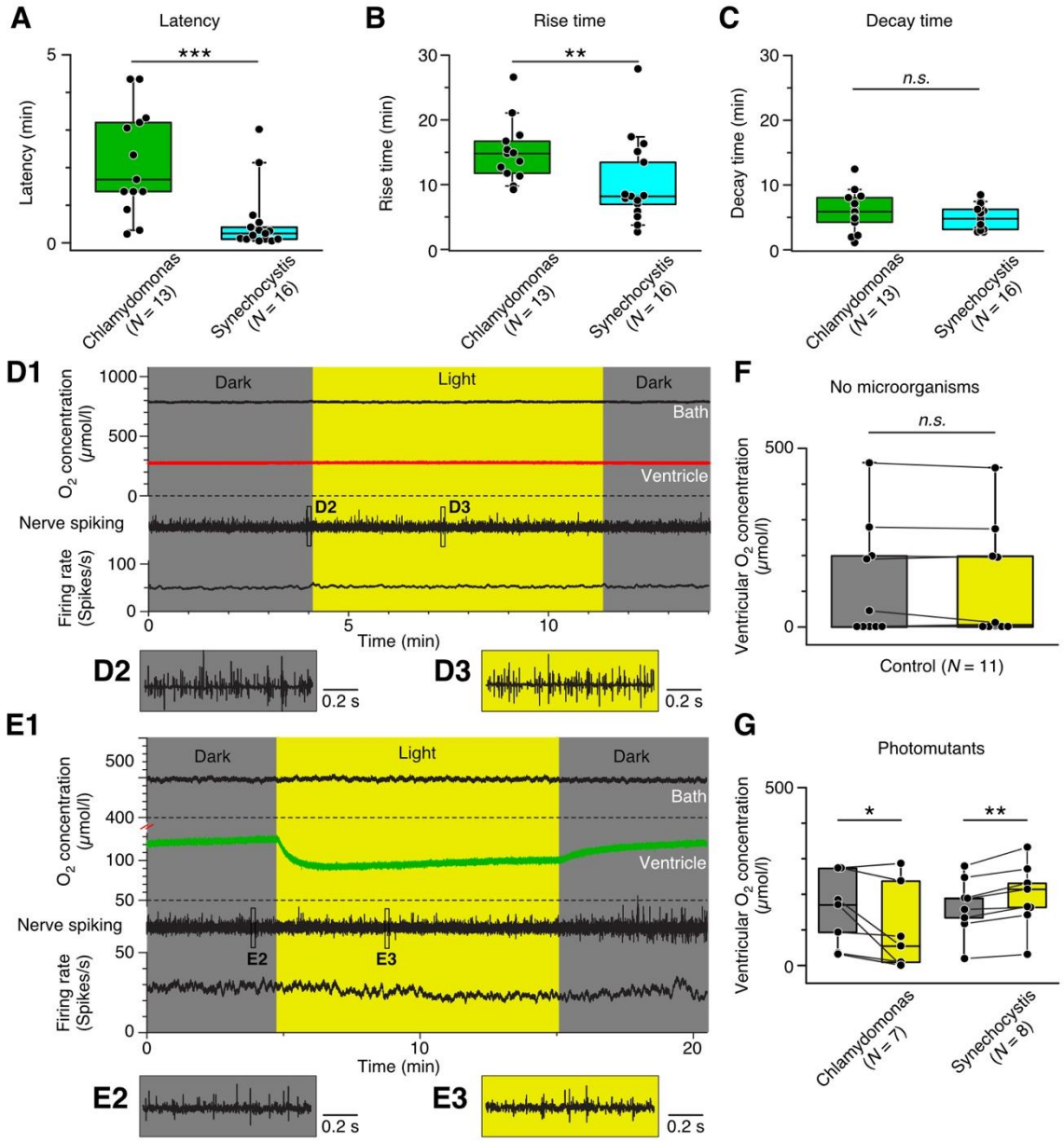

Supplemental fig. S2. Specificity of photosynthetic oxygen production (Related to Fig. 2). (**A, B, C**) Boxplots depicting latency (A), rise (B) and decay (C) times of light-induced increases in ventricular O_2 levels in preparations containing either *C. reinhardtii* or *Synechocystis* 6803; **, $p < 0.01$, ***, $p < 0.001$, Mann Whitney *U*-test. (**D, E**) Episodes (D1, E1) of O_2 concentration recordings in the bath chamber (black trace) and IVth ventricle (red and green trace in D, E) and of concurrent *superior oblique* nerve spiking and mean firing rate (black traces) in darkness and light in a preparation without microorganisms (D) and a preparation containing *C. reinhardtii* photomutants (E); in light, the ventricular O_2 concentration remains unaltered in the control (red trace in D) and even decreases in the preparation containing *C. reinhardtii* photomutants (green trace in E); insets show nerve spiking in darkness (D2, E2) and light (D3, E3) at higher temporal resolution. (**F, G**) Boxplots depicting ventricular O_2 concentrations in darkness (gray bars) and light (yellow bars) in preparations containing no microorganisms (F) or photomutants of *C. reinhardtii* or *Synechocystis* 6803 (G); *, $p < 0.05$, **, $p < 0.01$; Wilcoxon signed-rank test in F, G; *n.s.* not significant.

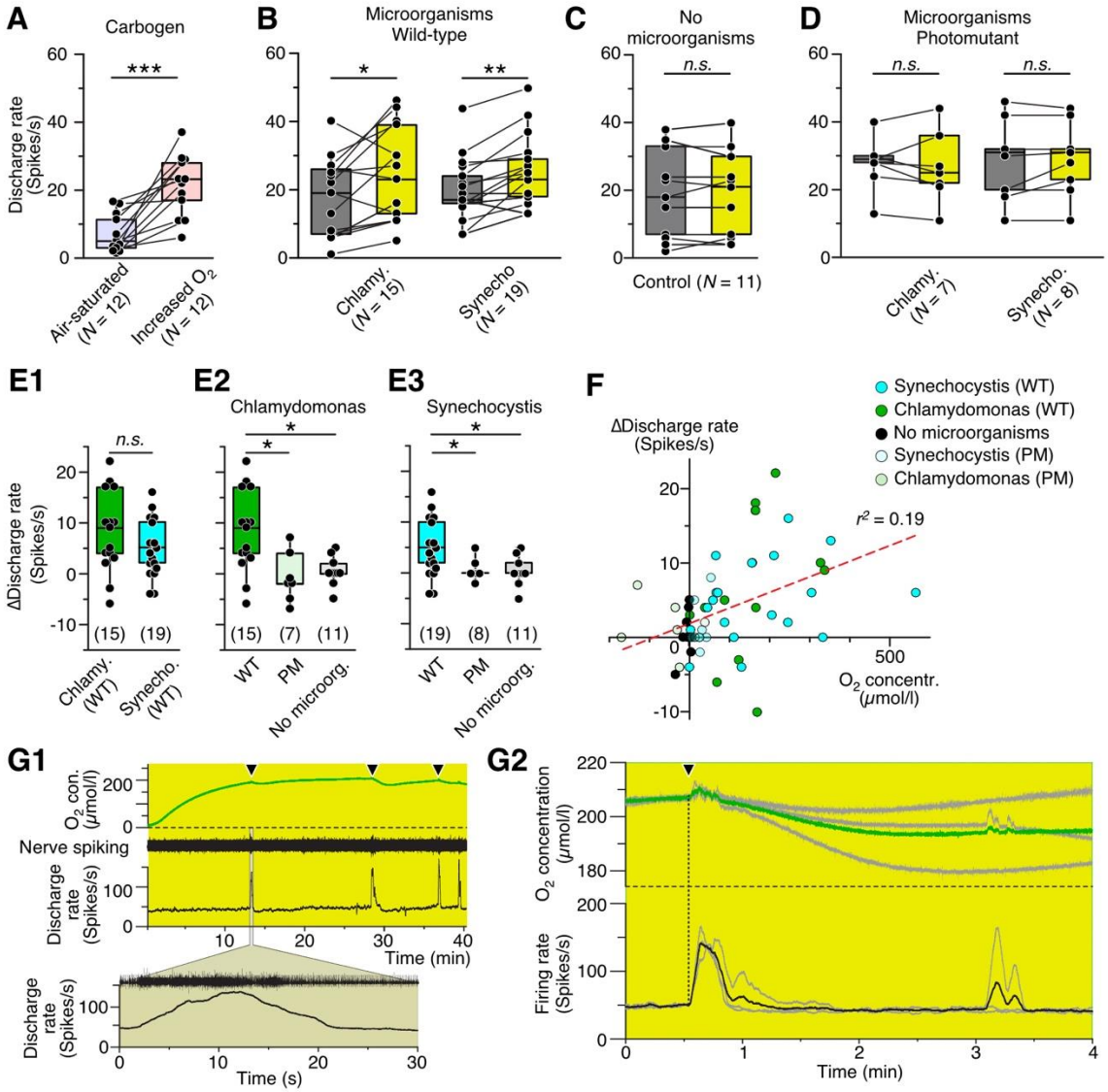

Supplemental fig. S3. Impact of enhanced oxygen concentration on neuronal discharge (Related to Fig. 2). (**A, B, C, D**) Boxplots depicting *superior oblique* nerve discharge rates at air-saturated (277 ± 3 µmol/l, mean ± sem) and carbogen-enhanced (803 ± 52 µmol/l, mean ± sem) bath O_2 levels (A) and in preparations with wild-type (WT) *C. reinhardtii* or *Synechocystis* 6803 (B), without microorganisms (C) and with photomutants of the two species (D) in darkness (gray bars) and light (yellow bars), respectively. (**E**) Boxplots depicting light-induced changes (Δ) of nerve discharge rates in preparations containing WT microorganisms (E1) in comparison with photomutants (PM) or controls without *C. reinhardtii* (E2) or *Synechocystis* 6803 (E3); number of experiments indicated in parentheses. *, $p < 0.05$, Mann Whitney *U*-test, Bonferroni-corrected; *n.s.* not significant. (**F**) Correlation between *superior oblique* nerve discharge rate changes (Δ) and ventricular O_2 concentration, revealing a significant linear dependency ($p < 0.0001$); (**G**) Ventricular O_2 concentration, nerve spiking and mean firing rate during illumination of a preparation with WT *C. reinhardtii* (G1); note that the O_2 level is transiently interrupted (▼ in G1) during spike bursts (inset below); overlays and average of transient interruptions of ventricular O_2 concentrations (gray and green traces) and mean firing rates (gray and black traces in G2) confirm the temporal match (dotted line) of the two parameters.